

DTIC FILE COPY

(4)

AFGL-TR-88-0155

AD-A200 620

PRODUCTION OF ATOMIC and MOLECULAR RADIATION BY ELECTRON IMPACT

Chun C. Lin

Department of Physics  
University of Wisconsin-Madison  
Madison, Wisconsin 53706

Final Report  
8 January 1987 - 8 June 1988

8 September 1988

Approved for public release; distribution unlimited

AIR FORCE GEOPHYSICS LABORATORY  
AIR FORCE SYSTEMS COMMAND  
UNITED STATES AIR FORCE  
HANSCOM AFB, MASSACHUSETTS 01731

DTIC  
ELECTE  
OCT 18 1988  
S D  
G  
H

38 10 18 104

"This technical report has been reviewed and is approved for publication"

*Edward T.P. Lee*

EDWARD T.P. LEE  
Contract Manager  
Atmospheric Effects Branch  
Optical/Infrared Technology Division

*Harold A. B. Gardiner for Robert R. O'Neil*

HAROLD A. B. GARDINER, Acting Chief  
Atmospheric Effects Branch  
Optical/Infrared Technology Division

FOR THE COMMANDER

*R. Earl Good*

R. EARL GOOD, Director  
Optical/Infrared Technology Division

This report has been reviewed by the ESD Public Affairs Office (PA) and is releasable to the National Technical Information Service (NTIS).

Qualified requestors may obtain additional copies from the Defense Technical Information Center. All others should apply to the National Technical Information Service.

If your address has changed, or if you wish to be removed from the mailing list, or if the addressee is no longer employed by your organization, please notify AFGL/DAA, Hanscom AFB, MA 01731. This will assist us in maintaining a current mailing list.

Unclassified

SECURITY CLASSIFICATION OF THIS PAGE (When Data Entered)

REPORT DOCUMENTATION PAGE		READ INSTRUCTIONS BEFORE COMPLETING FORM
1. REPORT NUMBER AFGL-TR-88-0155	2. GOVT ACCESSION NO. A200 620	3. RECIPIENT'S CATALOG NUMBER
4. TITLE (and Subtitle) Production of Atomic and Molecular Radiation by Electron Impact	5. TYPE OF REPORT & PERIOD COVERED Final 8 January 1987 - 8 June 1988	
	6. PERFORMING ORG. REPORT NUMBER	
7. AUTHOR(s) Chun C. Lin	8. CONTRACT OR GRANT NUMBER(s) F 19628-87-K0017	
9. PERFORMING ORGANIZATION NAME AND ADDRESS Department of Physics University of Wisconsin-Madison Madison, Wisconsin 53706	10. PROGRAM ELEMENT, PROJECT, TASK AREA & WORK UNIT NUMBERS 61102F 2310G4BX	
11. CONTROLLING OFFICE NAME AND ADDRESS Air Force Geophysics Laboratory Hanscom AFB, Massachusetts 01731 Monitor/Edward T. P. Lee/LSI	12. REPORT DATE 8 September 1988	
	13. NUMBER OF PAGES 46	
14. MONITORING AGENCY NAME & ADDRESS (if different from Controlling Office)	15. SECURITY CLASS. (of this report) Unclassified	
	15a. DECLASSIFICATION/DOWNGRADING SCHEDULE	
16. DISTRIBUTION STATEMENT (of this Report) Approved for public release; distribution unlimited		
17. DISTRIBUTION STATEMENT (of the abstract entered in Block 20, if different from Report)  a 1 P-102		
18. SUPPLEMENTARY NOTES  c' sub 4		
19. KEY WORDS (Continue on reverse side if necessary and identify by block number) c' <sub>4</sub> → a emission of N <sub>2</sub> molecules, optical emission cross sections, Franck-Condon factors, emission lines of O <sup>+</sup> ions.		
20. ABSTRACT (Continue on reverse side if necessary and identify by block number) - Electron-impact excitation cross sections of the c' <sub>4</sub> <sup>1</sup> Σ <sub>u</sub> <sup>+</sup> → a <sup>1</sup> Π <sub>g</sub> emission bands of N <sub>2</sub> <sup>m</sup> molecules involving different vibrational quantum numbers <sup>g</sup> has been measured. Excitation of the vibrational levels of the c' <sub>4</sub> <sup>1</sup> state is analyzed in terms of the Franck-Condon factors and perturbation by the b' <sub>4</sub> <sup>1</sup> Σ <sub>u</sub> <sup>+</sup> state. Nonlinearity in the pressure dependence of the emission signal is studied. Optical cross sections have been measured for emission lines of O <sup>+</sup> ions produced by electron impact on O <sub>2</sub> <sup>m</sup> molecules.		

DD FORM 1473

EDITION OF 1 NOV 65 IS OBSOLETE

Unclassified

SECURITY CLASSIFICATION OF THIS PAGE (When Data Entered)

TABLE OF CONTENTS

	<u>PAGE</u>
Electron-Impact Excitation of the Vibrational Levels of the $c_4^1 \Sigma_u^+$ State of the Nitrogen Molecule	1
References	11
Further Studies of Electron-Impat Excitation of the Electronic States of Nitrogen Molecules	13
References	28
Emission of Atomic Oxygen Ions Radiation Produced by Electron Impact on Oxygen Molecules	29
References	41
Publications	42



<b>Accession For</b>	
NTIS GRA&I	<input checked="" type="checkbox"/>
DTIC TAB	<input type="checkbox"/>
Unannounced	<input type="checkbox"/>
Justification	
By _____	
Distribution/	
<b>Availability Codes</b>	
Dist	Avail and/or Special
A-1	

Part I

ELECTRON-IMPACT EXCITATION OF THE VIBRATIONAL LEVELS OF THE  $c_4^1 \Sigma_u^+$   
ELECTRONIC STATE OF THE NITROGEN MOLECULE

Electron-impact excitation of the  $c_4^1 \Sigma_u^+$  state of the  $N_2$  molecule has received considerable attention in the literature. One aspect of the interest is that  $c_4^1 \Sigma_u^+$  is a Rydberg state whereas most of the previous optical studies of electron-impact experiments dealt with excitation to the valence-type electronic states.<sup>1</sup> Also, because of the  $c_4^1 \Sigma_u^+ \rightarrow a^1 \Pi_g$  emission, electron-impact excitation of  $c_4^1 \Sigma_u^+$  may have a significant influence on the population of  $a^1 \Pi_g$  which is an infrared emitting state ( $a^1 \Pi_g \rightarrow a'^1 \Sigma_u^-$ ).<sup>2</sup> Moreover comparison of the  $c_4^1 \Sigma_u^+ \rightarrow a^1 \Pi_g$  with the  $c_4^1 \Sigma_u^+ \rightarrow X^1 \Sigma_g^+$  intensities in auroral emission has raised an interesting issue in the spectra of the upper atmosphere.<sup>3,4</sup> In an earlier paper Filippelli *et al.* measured optical emission cross sections for electron-impact excitation of the  $c_4^1 \Sigma_u^+(v'=0) \rightarrow a^1 \Pi_g(v'')$  bands with  $v''$  from 0 through 5, but cross sections for  $v' \neq 0$  were not obtained because of the lower emission intensity. In the present work we report a systematic study of the cross sections of the  $c_4^1 \rightarrow a$  bands with  $v' \neq 0$ .

The apparatus and the procedure for measuring optical emission cross sections for molecular bands has been described in Ref. 1. A schematic diagram of the apparatus is shown in Fig. 1. Inside the collision chamber a collimated monoenergetic electron beam of diameter about 3 mm passes through  $N_2$  gas (research grade) at a pressure of 10 mTorr or less. The electron beam is collected by a Faraday cup (not shown in the figure) and the beam current measured by an electrometer. The  $c_4^1 \rightarrow a$  radiation emitted from a small segment of the electron beam (P in Fig. 1) is observed perpendicular to the beam axis (XX') through a slot cut into the wall of the Faraday cup and a window W. The

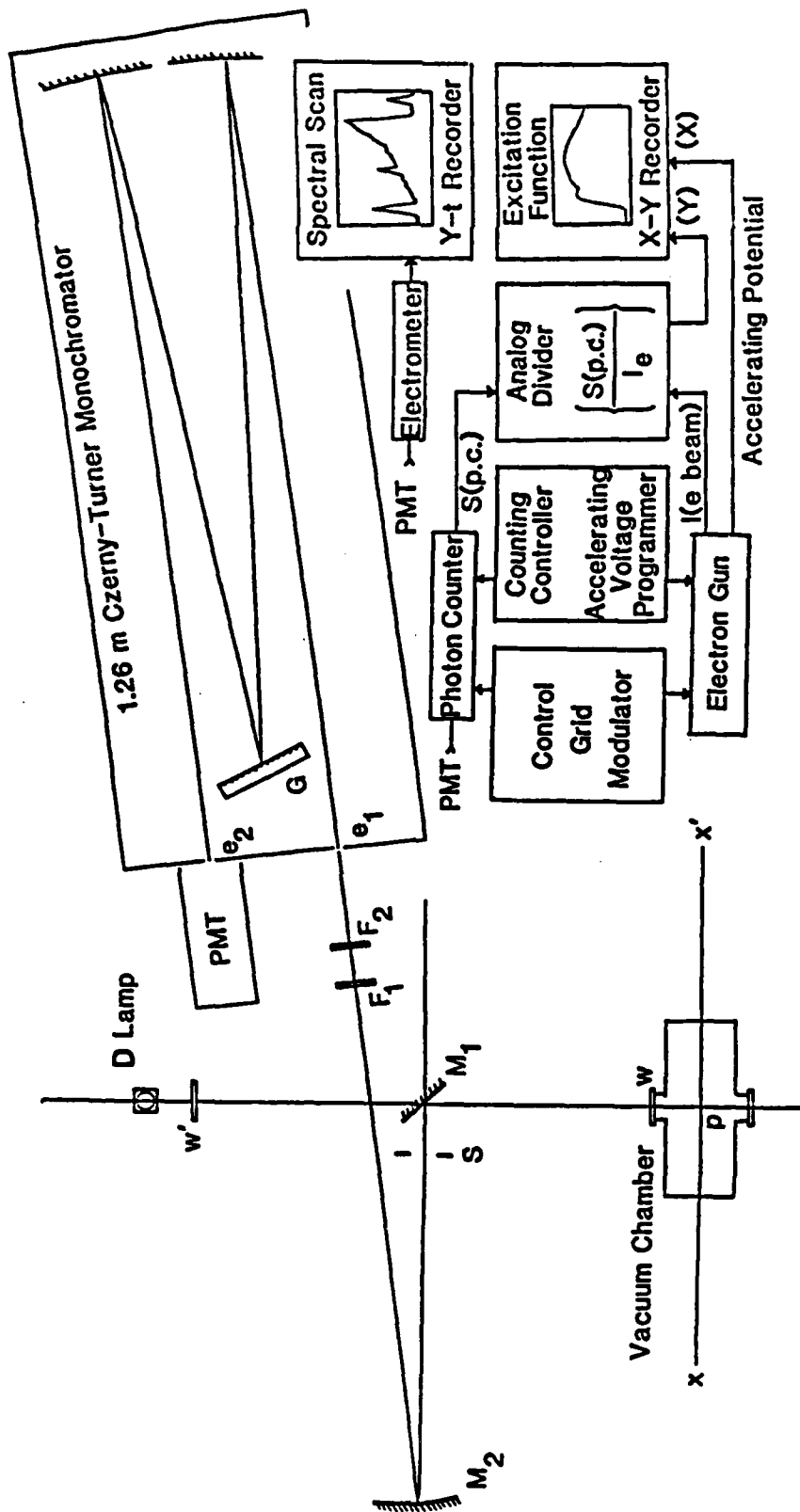


Figure 1. Schematic diagram of the apparatus for measuring electron-impact optical emission cross sections.

emerging light passes through the monochromator and is detected by a photomultiplier (EMI 9789QA in this experiment). The solid angle viewed by the monochromator is defined by the circular stop S. The photomultiplier output is fed to either an electrometer or a photon counter. The  $N_2$  gas pressure in the collision chamber is measured with an MKS Baratron capacitance manometer. The local gas heating effect discussed in Ref. 1 is taken into account in determining the  $N_2$  number density. For absolute calibration of the emission intensity, the collision chamber is replaced with a deuterium standard lamp (Optronics Laboratories Model UV-40) of known spectral irradiance. This is done by rotating mirror  $M_1$  through  $90^\circ$  to allow radiation from the standard lamp to enter the monochromator. The resulting photomultiplier signal is recorded as a function of wavelength. A silica plate  $W'$  is placed on the optical path of the standard lamp in order to compensate for the collision chamber window  $W$  of the same thickness. From the measured quantities in these experiments, the optical cross sections are determined by using Eq.(7) of Ref. 1. No polarization correction is made because the polarization effect is expected to be very small as explained in Ref. 1.

We have scanned the emission spectrum from the collision chamber over the wavelength range of 2,000-3670 Å which covers all the  $(v',v'')$  bands of the  $c'_4 \rightarrow a$  electronic transition with  $v'=0-4$  and  $v''=0-5$ . While we have observed emission signals in the wavelength regions corresponding to the  $c'_4 \rightarrow a(v',v'')$  bands for  $0 \leq v' \leq 4$  and  $0 \leq v'' \leq 5$ , most of the bands with  $v' \neq 0$  are contaminated by  $N_2$  emission bands of other systems. The (4,0) and (4,1) bands, however, are sufficiently free from other bands to allow unambiguous determination of the emission cross sections. The peak excitation cross sections for optical emission of the (4,0) and (4,1) bands are  $0.20 \times 10^{-20}$  and  $0.34 \times 10^{-20} \text{ cm}^2$  respectively. The excitation function for both bands exhibits the broad-peak

shape similar to that of the (0,0) band reported in Ref. 1. In Fig. 2 is shown the optical emission excitation functions of the (4,0) and (4,1) bands as compared to that of the (0,0) band. The (1,2) band is strongly overlapped by the  $D^2\Pi_g \rightarrow A^2\Pi_u$  (7,8) band of  $N_2^+$ . The latter has a threshold excitation energy of 22 eV which is considerably larger than the 13-eV threshold of  $c_4^+ \rightarrow a$ , and is expected to have a slow rising excitation function characteristic of simultaneous ionization-excitation by electron impact.<sup>5</sup> Thus it is possible to minimize the interference of the  $D^2\Pi_g \rightarrow A^2\Pi_u$  band by measuring the emission cross sections at low energies and use the excitation function of Fig. 2 to extrapolate to higher energies. In this way we obtain the peak cross section for the (1,2) band as  $0.03 \times 10^{-20} \text{ cm}^2$ . Even excluding the D+A (7,8) band, there is a nearby  $b^1\Pi_g \rightarrow a^1\Pi_g$  (5,1) band and a  $N_2^+ B^2\Sigma_u^+ \rightarrow X^2\Sigma_g^+$  (21,12) band which must be subtracted from the observed signal in order to isolate the (1,2) emission. We estimate that the uncertainty of the cross section of the (1,2) band could be as large as 90% because of this subtraction and the very low signal level. For the (4,0) and (4,1) cross sections our estimated uncertainties are 37% and 28% respectively.

The peak cross sections of the (1,2), (4,0), and (4,1) bands are much smaller than those of the (0, $v''$ ) bands which are  $1.30 \times 10^{-20}$ ,  $3.16 \times 10^{-20}$  and  $2.23 \times 10^{-20} \text{ cm}^{-2}$  for  $v'' = 0, 1, \text{ and } 2$  respectively. Direct electron-impact cross sections for excitation of the  $c_4^+ \ ^1\Sigma_u^+(v')$  vibrational levels from the ground level  $X^1\Sigma_g^+(v=0)$  have been given by Zipf and McLaughlin<sup>6</sup> as  $1.58 \times 10^{-17}$ ,  $1.45 \times 10^{-19}$ ,  $1.34 \times 10^{-18}$ , and  $3.84 \times 10^{-18} \text{ cm}^2$  at 200 eV for  $v'=0, 1, 3$  and 4 respectively. By far the major radiative decay channel for the  $c_4^+$  state is the  $c_4^+ \rightarrow X$  emission; the intensity of the  $c_4^+ \rightarrow a$  emission is about two orders of magnitude lower than that of  $c_4^+ \rightarrow X$ . Only a very small fraction of the molecules in the  $c_4^+ \ ^1\Sigma_u^+(v')$  level is responsible for the  $c_4^+ \rightarrow a(v', v'')$  emission.

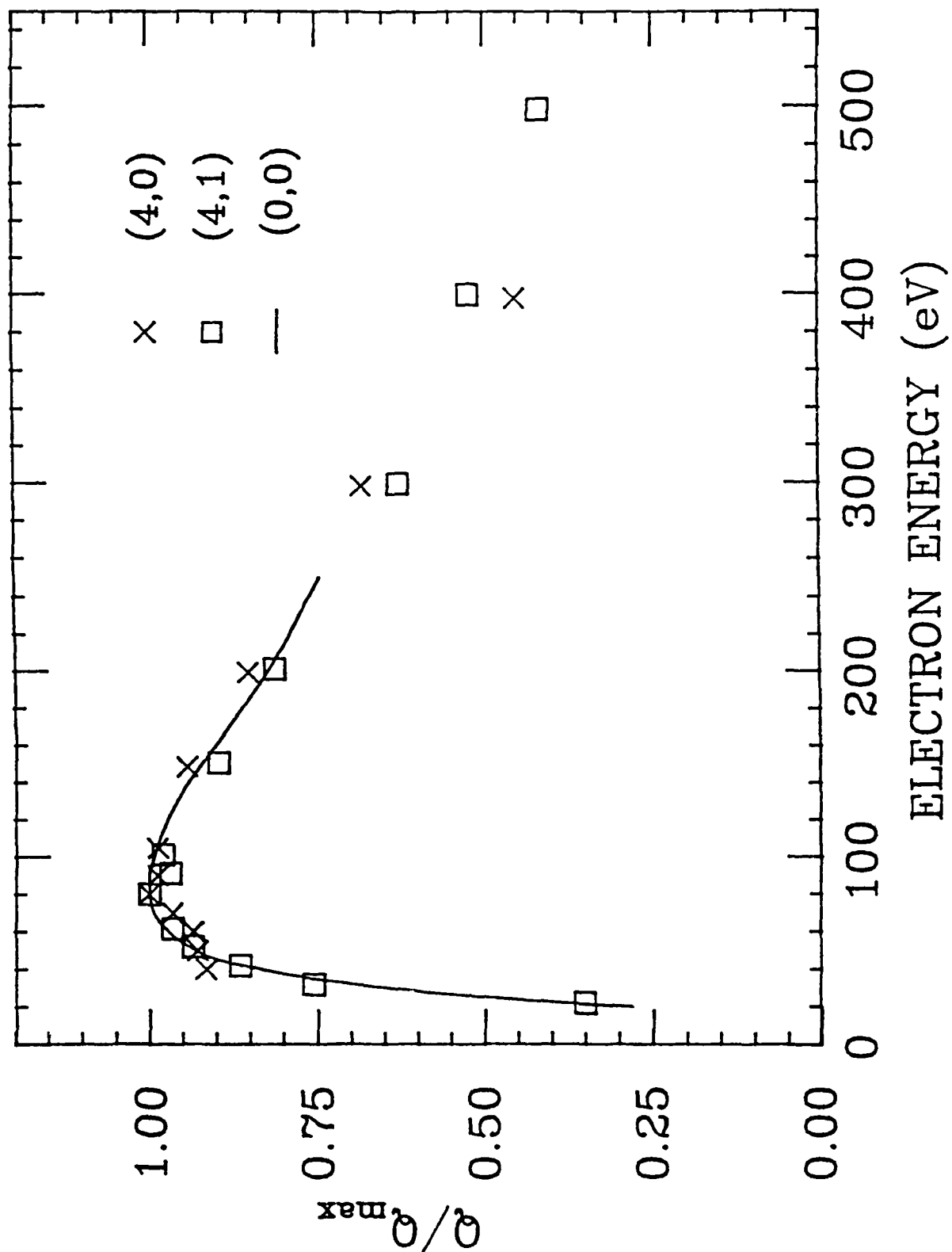


Figure 2. Excitation functions of the (4,0) and (4,1) bands of the  $c'_4 \rightarrow a$  transition as compared to the excitation function of the (0,0) band.

Our measured optical emission cross sections of  $c_4 \rightarrow a(v', v'')$  are indeed much smaller than the direct excitation cross sections of the  $c_4(v')$  level cited above. The optical emission cross section of  $c_4 \rightarrow a(v', v'')$  is related to the population of the  $c_4(v')$  level and the branching ratio of the transition involved. The population of the  $c_4(v')$  level is dictated not only by direct electron-impact excitation from the ground electronic-vibrational level  $X^1\Sigma_g^+(v=0)$  but also by cascade from the higher levels. Nevertheless we can expect a qualitative correlation of the direct excitation cross section of the  $c_4(v')$  level,  $Q_{dir}[c_4(v')]$ , with the optical emission cross sections,  $Q_{opt}[c_4 \rightarrow a(v', v'')]$ , although there is no simple proportionality relation between the two sets of cross sections. Indeed we observe the same trend in the variation of the cross section with  $v'$  for  $Q_{dir}$  and  $Q_{opt}$ , namely, the cross sections for  $v'=0$  are much larger than those for  $v'=4$  which in turn are much larger than those for  $v'=1$ .

To further study the excitation of the various vibrational levels of the  $c_4^1\Sigma_u^+$  state, we calculate the relevant  $X^1\Sigma_g^+(v=0) \rightarrow c_4^1\Sigma_u^+(v')$  Franck-Condon factors for excitation from the  $X^1\Sigma_g^+(v=0)$  ground level. The potential curve for  $X^1\Sigma_g^+$  is well known. Since some of the  $c_4$  levels are perturbed, it may not be appropriate to describe all the vibrational levels with a single potential function. Nevertheless we will first adopt such a single potential description, and discuss the perturbation of the  $c_4$  state later. To construct the potential curve for the  $c_4$  state, we use the listing of classical turning points ( $r_{max}$  and  $r_{min}$ ) for  $v'=0$  through 8 in the article of Lofthus and Krupenie.<sup>7</sup> The rest of the potential curve is obtained by fitting these points to a Morse's potential with the proper dissociation limit. If there were no avoided level crossing, the  $c_4^1\Sigma_u^+$  state, being a Rydberg one, would connect to the  $N(2p^3) + N(2p^2 3p)$  manifold at infinite internuclear distance. With avoided

crossing the  $c_4^1 \Sigma_u^+$  state probably has a dissociation limit of  $N(2p^3 \ ^2D) + N(2p^3 \ ^2P)$ . The calculated vibrational wave functions of  $c_4^1 \Sigma_u^+(v' \leq 4)$  are found to be virtually the same for either dissociation limit because these low vibrational levels are not influenced by the part of the potential curve outside the classical region of the  $v'=8$  state. The Franck-Condon factors for  $X^1 \Sigma_g^+(v=0) \rightarrow c_4^1 \Sigma_u^+(v')$  are 0.93, 0.065,  $3.6 \times 10^{-3}$ ,  $3.5 \times 10^{-4}$ , and  $5.9 \times 10^{-5}$  for  $v'=0, 1, 2, 3$ , and 4 respectively. As an alternative, a second potential is generated by constructing a Morse's potential based on the spectroscopic data  $r_e$ ,  $\omega_e$ , and  $\omega_e x_e$  which completely specify the Morse function.<sup>8</sup> This potential should be accurate for the very low vibrational states, but much less reliable for dissociation energy. The five Franck-Condon factors ( $v'=0-4$ ) derived from this potential are 0.97, 0.033,  $6.7 \times 10^{-4}$ ,  $5.0 \times 10^{-5}$ , and  $1.05 \times 10^{-5}$ . In both sets the (0,0) Franck-Condon factor is unusually close to unity. This happens because the  $X^1 \Sigma_g^+$  and  $c_4^1 \Sigma_u^-$  states have very similar  $r_e$  (1.098 and 1.108 Å) and  $\omega_e$  (2359 and 2202  $\text{cm}^{-1}$ ). Thus the vibrational wave function of  $X(v=0)$  is nearly identical to that of  $c_4^1(v'=0)$ , and is nearly orthogonal to those of  $c_4^1(v' \neq 0)$ . This near orthogonality makes the other four Franck-Condon factors very small and sensitive to the choice of the potential as reflected by the two sets of numbers above. To check whether the direct cross sections of exciting  $c_4^1(v')$  from the  $X^1 \Sigma_g^+(v=0)$  ground level given in Ref. 6 conform to the Franck-Condon factors, we find the cross section ratio between  $v'=1$  and  $v'=0$  as 0.00918 according to the experimental results (Ref. 6) whereas the corresponding ratio of the Franck-Condon factors derived from the two different potentials used above are 0.070 and 0.034. We prefer 0.034 over 0.070 since the former is generated from a  $c_4^1$  potential that is better suited for the very low vibrational levels. In view of the sensitivity of the (0,1) Franck-Condon factor to the choice of potential, we regard the relative direct cross sections

of  $c_4^+(v'=0)$  and  $c_4^+(v'=1)$  as being in reasonable accord with the Franck-Condon factor. This, however, is not the case for the higher- $v'$  levels. Based on the Franck-Condon approximation, the direct cross section  $Q_{dir}[c_4^+(v'=0)]$  is expected to be more than four orders of magnitude larger than that for  $v'=4$ , whereas experimentally the ratio is only 4:1. Even more striking is the ratio of  $Q_{dir}[c_4^+(v'=4)]$  to  $Q_{dir}[c_4^+(v'=1)]$  which, according to the Franck-Condon description, should be of the order of  $10^{-3}$  in drastic disagreement with the experimental value of 26. Our optical measurements also show much larger emission cross sections for  $v'=4$  than  $v'=1$  agreeing at least qualitatively with the direct excitation experiment. This vast deviation from the Franck-Condon picture can be attributed to the perturbation arising from the interaction between the  $c_4^+ \ ^1\Sigma_u^+$  and  $b' \ ^1\Sigma_u^+$  states.<sup>9</sup> As pointed out earlier, the vibrational wave function of  $c_4^+(v'=4)$  is nearly orthogonal to that of the  $X(v=0)$  ground state. This orthogonality would be spoiled by the admixture of  $c_4^+(v'=4)$  with  $b'(v')$  if the vibrational wave functions of the latter have appreciable amplitudes in the range of internuclear distance corresponding to the Franck-Condon region of the  $X(v=0)$  ground state (1.055 to 1.145 Å). The  $c_4^+(v'=4)$  level is nearly degenerate with  $b'(v'=13)$ , and inspection of the potential curve<sup>9</sup> shows that the vibrational wave function of  $b'(v'=13)$  does penetrate into the Franck-Condon region of  $X(v=0)$ . Thus the  $b'(v'=13)$  component in the perturbed  $c_4^+(v'=4)$  state may be responsible for the observed cross section for direct excitation from the  $X(v=0)$  ground state. The same kind of perturbation also applies to  $c_4^+(v'=1)$  which is nearly degenerate with  $b'(v'=4)$ . The classical vibrational span of internuclear distance for the  $b'(v'=4)$  state, however, is well outside the Franck-Condon region of the  $X(v=0)$  ground state. Thus the direct electron-impact cross section remains small for excitation from  $X(v=0)$  to a state that is a mixture of  $c_4^+(v'=1)$  and  $b'(v'=4)$ .

Filippelli et al. reports a non-linear pressure dependence of the  $c_4 \rightarrow a$  (0,0) intensity at pressures above 0.1 mTorr.<sup>1</sup> This occurs because the major radiative decay channel of  $c_4(v'=0)$  is the  $c_4 \rightarrow X(0,0)$  emission on account of the much larger transition probability of  $c_4 \rightarrow X$  over  $c_4 \rightarrow a$  and of the very favorable Franck-Condon factor (nearly equal to 1) between  $c_4(v'=0)$  and  $X(v''=0)$ . When the  $c_4 \rightarrow X(0,0)$  radiation is re-absorbed by the  $X(v=0)$  ground-state molecules, the resulting  $c_4(v'=0)$  molecules have a probability of decaying into the  $a(v'')$  level instead of returning to  $X(v=0)$ . Thus the  $c_4 \rightarrow (0, v'')$  emission intensity is enhanced by the re-absorption process resulting in a non-linear pressure dependence. For the  $c_4 \rightarrow a(4,0)$  and  $c_4 \rightarrow a(4,1)$  emission studied in the present paper, one may expect the same kind of non-linear pressure dependence. However, the  $c_4 \rightarrow X(4, v'')$  radiation is distributed over different  $v''$  and not confined chiefly to  $v''=0$  in contrast to the case of  $c_4 \rightarrow X(0, v'')$ . Since the population of the  $X(v'' \neq 0)$  levels are much lower than that of  $X(v''=0)$ , the  $c_4 \rightarrow X(4, v'' \neq 0)$  emission is only very weakly re-absorbed in comparison with  $c_4 \rightarrow X(4,0)$ . Thus the re-absorption enhancement for  $c_4 \rightarrow a(4,0)$  and  $c_4 \rightarrow a(4,1)$  is less than that for  $c_4 \rightarrow a(0,0)$ . This is indeed reflected in our data as non-linear pressure dependence for the  $c_4 \rightarrow a(4,1)$  intensity is found to be negligible at pressures below 0.5 mTorr. We expect an even weaker non-linear pressure dependence for the  $c_4 \rightarrow a(1,2)$  intensity because of the unfavorable Franck-Condon factor for the  $c_4 \rightarrow X(1,0)$  emission which is responsible for re-absorption from the ground electronic-vibrational level. However, the  $c_4 \rightarrow a(1,2)$  emission is too weak to make a systematic study of the pressure effect.

No direct excitation cross section was given for the  $c_4(v=2)$  state in Ref. 6. In our experiment we found radiation signal at the wavelengths of the (2,0), (2,1), (2,2), (2,3), (2,4), and (2,5) bands of  $c_4 \rightarrow a$ . However, in all

cases there are other  $N_2$  band systems in the same wavelength regions making it difficult to isolate the  $c_4 \rightarrow a(2, v'')$  emission cross sections. The same is also true for the  $c_4 \rightarrow a(3, v'')$  series.

In summary we have compared the electron-impact excitation of the vibrational levels ( $v'=0, 1, 4$ ) of the  $c_4$  electronic state of  $N_2$ . Because the equilibrium internuclear distance and energy curve of the  $c_4$  state are similar to their counterpart of the X state, electron-impact excitation from  $X(v=0)$  to  $c_4(v=1)$  is much less favorable than to  $c_4(v=0)$  on account of the very large difference between the relevant Franck-Condon factors. The observed excitation cross sections for  $c_4(v'=4)$ , however, are several orders of magnitudes larger than expected from consideration of the Franck-Condon principle. This is attributed to the perturbation of the  $c_4(v=4)$  state by admixture of the  $b'(v')$  states, especially  $v'=13$ .

#### REFERENCES

1. A. R. Filippelli, S. Chung and C. C. Lin, Phys. Rev. A 29, 1709 (1984).
2. W. J. Marinelli, B. D. Green, M. A. DeFaccio, W. A. M. Blumberg, J. Phys. Chem. 92, 3429 (1988).
3. T. G. Slanger, Planet. Space Sci. 31, 1525 (1983).
4. T. G. Slanger, Planet. Space Sci. 34, 399 (1986).
5. R. M. St. John and C. C. Lin, J. Chem. Phys. 41, 195 (1964).
6. E. C. Zipf and R. W. McLaughlin, Planet. Space Sci. 26, 449 (1978).
7. A. Lofthus and P. H. Krupenie, J. Phys. Chem. Ref. Data 6, 113 (1977).
8. K. P. Huber and G. Herzberg, Molecular Spectra and Molecular Structure IV. Constants of Diatomic Molecules (Van Nostrand Reinhold Company, New York 1979).
9. K. Dressler, Can. J. Phys. 47, 547 (1969).

## Part II

### FURTHER STUDIES OF ELECTRON-IMPACT EXCITATION OF THE ELECTRONIC STATES OF NITROGEN MOLECULES

In their study of electron-impact excitation of the  $c_4^+ \rightarrow a(0,0)$  band, Filippelli et al. pointed out the nonlinearity in the pressure dependence of the  $c_4^+ \rightarrow a(0,0)$  signal produced by electron impact on  $N_2$ .<sup>1</sup> They attributed this nonlinearity to reabsorption of the  $c_4^+ \rightarrow a(0,0)$  by the  $N_2$  molecules in the ground electronic-vibrational state, but no measurement of the degree of nonlinearity was made.

To study this nonlinearity effect quantitatively we have measured the  $c_4^+ \rightarrow a(0,0)$  emission at a series of gas pressure and electron beam current. To exhibit the nonlinear pressure dependence we plot the ratio of the photomultiplier tube (PMT) signal to pressure (S/P) versus pressure up to 2.5 mTorr. In Figure 3 we show these plots at three different beam currents (50 $\mu$ A, 100 $\mu$ A, 150 $\mu$ A) with electron energy at 50 eV. The data points are found to fit approximately the simple relation

$$\frac{S}{P} = a + bP. \quad (\text{II-1})$$

Similar plots for electron energies of 80 eV and 150 eV are shown in Figs. 4 and 5 respectively. The values of the ratio b/a at various beam currents and electron energies are given in Table I. We see that this ratio does not vary much for the entire range of beam current and electron energy studied. In Figs. 6-8 we show the value of a at three different electron energies as a function of the beam current. The linearity is expected of

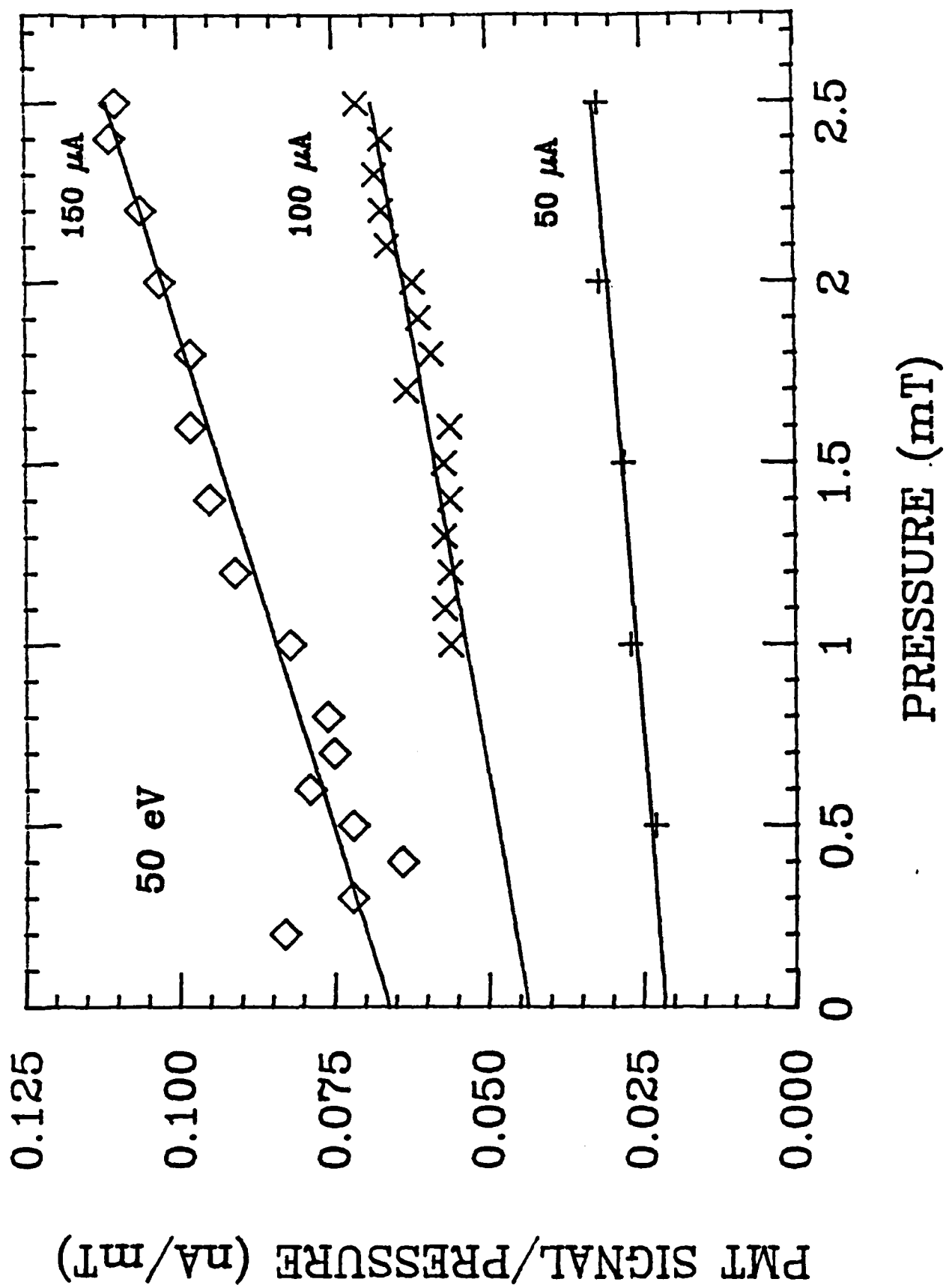


Figure 3. Plot of S/P versus pressure at 50 eV.

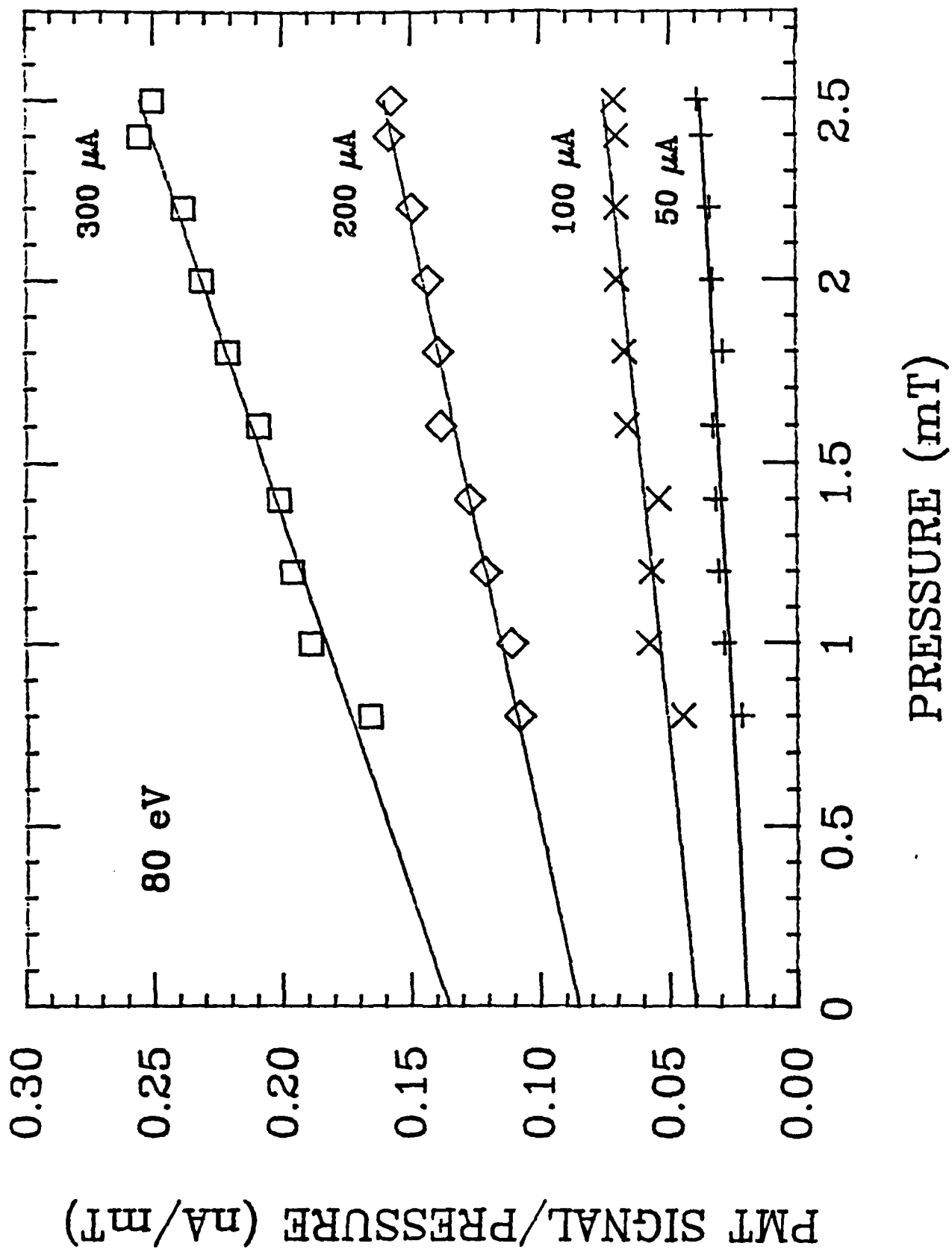


Figure 4. Plot of S/P versus pressure at 80 eV.

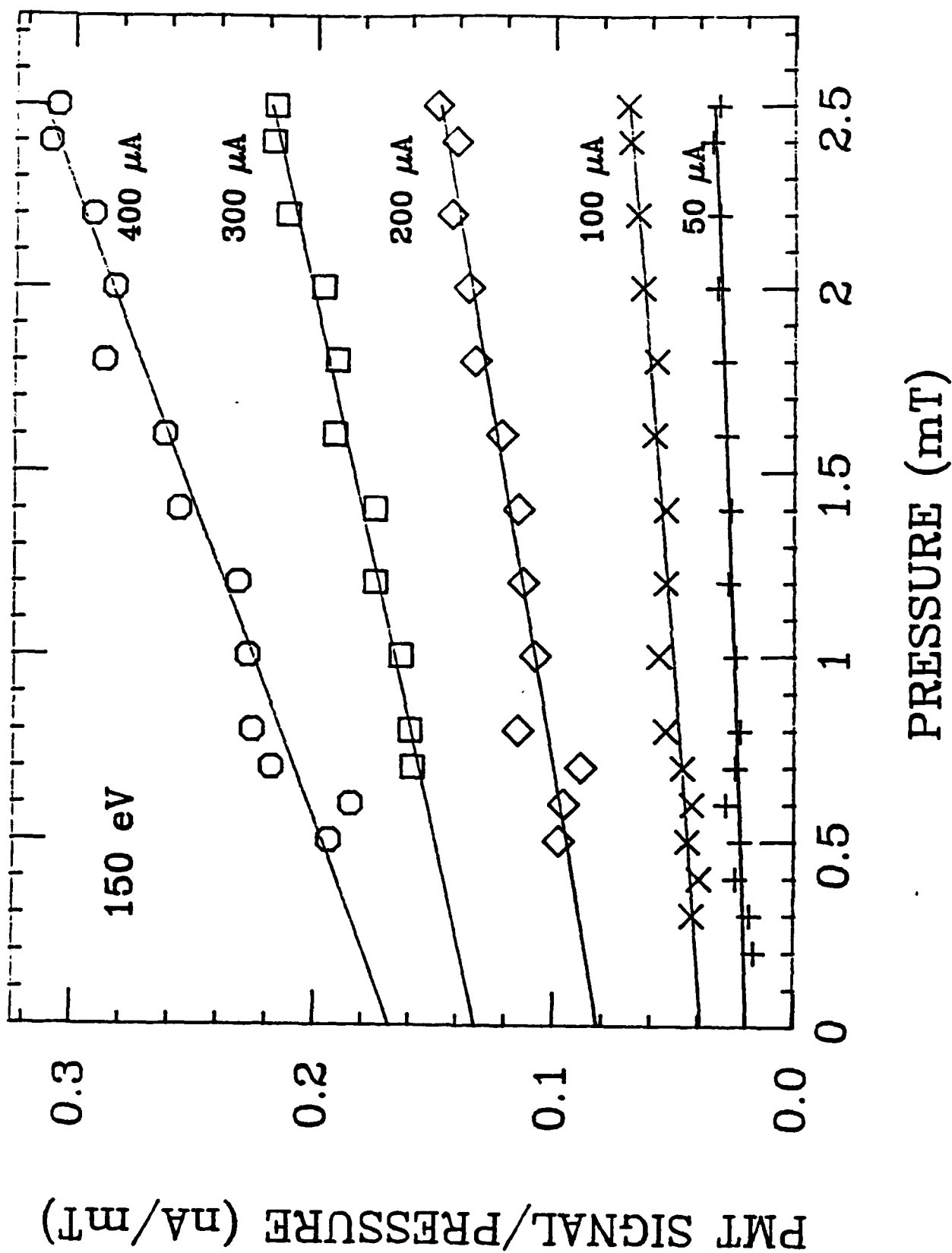


Figure 5. Plot of S/P versus pressure at 150 eV.

Table I. The ratio of  $b/a$  as defined in Eq.(II-1) determined at different values of electron energy ( $E$ ) and electron beam current ( $I_e$ ).

$I_e$ ( $\mu A$ )	Values of $b/a$			
	$E = 50$ eV	$E = 80$ eV	$E = 100$ eV	$E = 150$ eV
50	0.214	0.345		0.285
100		0.338		0.320
150	0.275			
200		0.341		0.326
300		0.354		0.263
350			0.312	
400				0.345

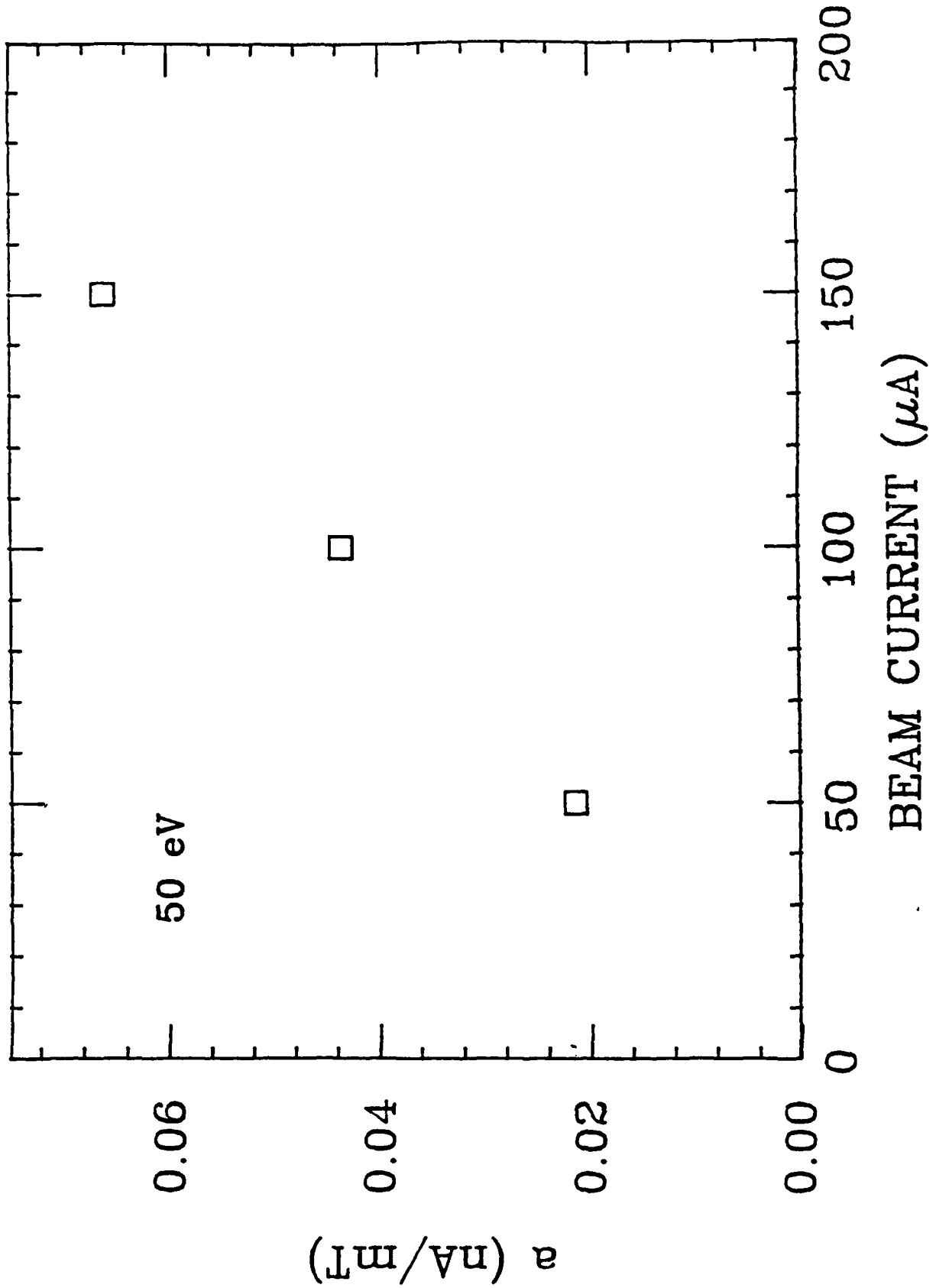


Figure 6. Plot of coefficient a versus beam current at 50 eV.

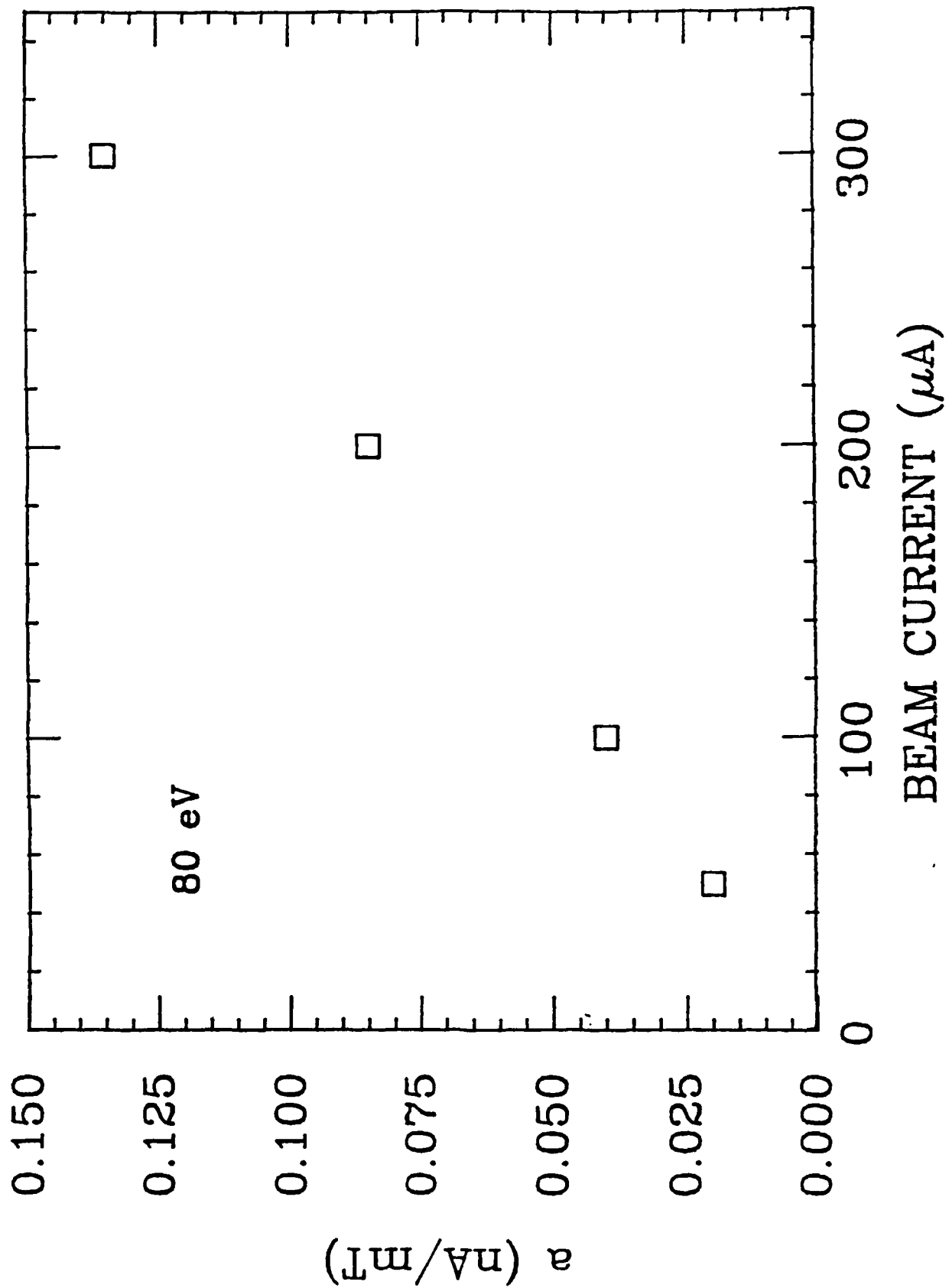


Figure 7. Plot of coefficient  $a$  versus beam current at 80 eV.

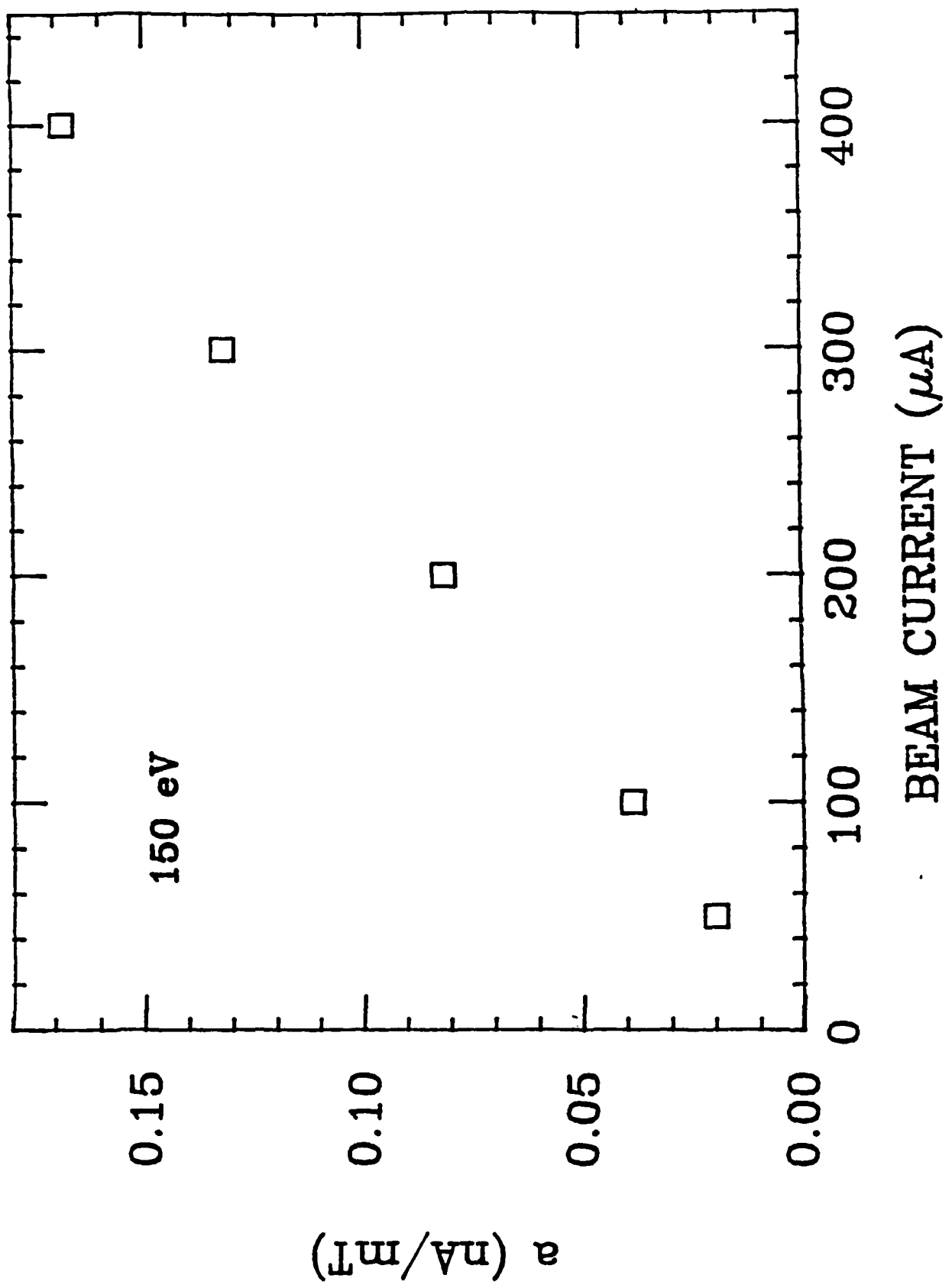


Figure 8. Plot of coefficient  $a$  versus beam current at 150 eV.

single-electron collision processes. The relation between  $b$  and the beam current as shown in Figs. 9-11, however, appears to conform not quite as well to a linear function.

Another interesting question about electron excitation of the  $c_4 \rightarrow a$  emission is whether a substantial part of the population of the  $c_4$  state is due to cascade from the higher states. If these higher states (cascading states) have lifetime very different from that of the  $c_4$  state, then a measurement of decay curve (emission intensity as a function of time after turning off the electron beam) should reveal a mixture of different lifetimes. The lifetime of the  $c_4$  state is about 0.9 nsec,<sup>2</sup> thus very high time-resolution is needed to determine the lifetimes of the different decay modes. A simpler approach is to measure the  $c_4 \rightarrow a$  emission intensity profile of the electron beam, i.e., the variation of the emission intensity of the  $c_4 \rightarrow a$  bands as a function of the radial distance from the center of the beam. If the  $c_4$  level receives no cascade, the excited  $N_2(c_4)$  molecules can move only a very short distance before decaying away because of the very short lifetime. However, if the  $c_4$  level is populated significantly by cascade from a higher level with a much longer lifetime, then it is possible to have some  $c_4 \rightarrow a$  radiation "outside" the electron beam. This would have the effect of broadening the profile of the  $c_4 \rightarrow a$  radiation. To measure the intensity profile we place a vertically translatable horizontal slit of width 0.397 mm in front of the monochromator entrance slit and measure the  $c_4 \rightarrow a(0,0)$  signal as a function of the vertical position of the horizontal slit. The measured emission signal plotted as a function of the slit position is shown in Fig. 12. The data points were obtained at a gas pressure of 7.7 mTorr, an electron beam current of 200  $\mu$ A, and an electron

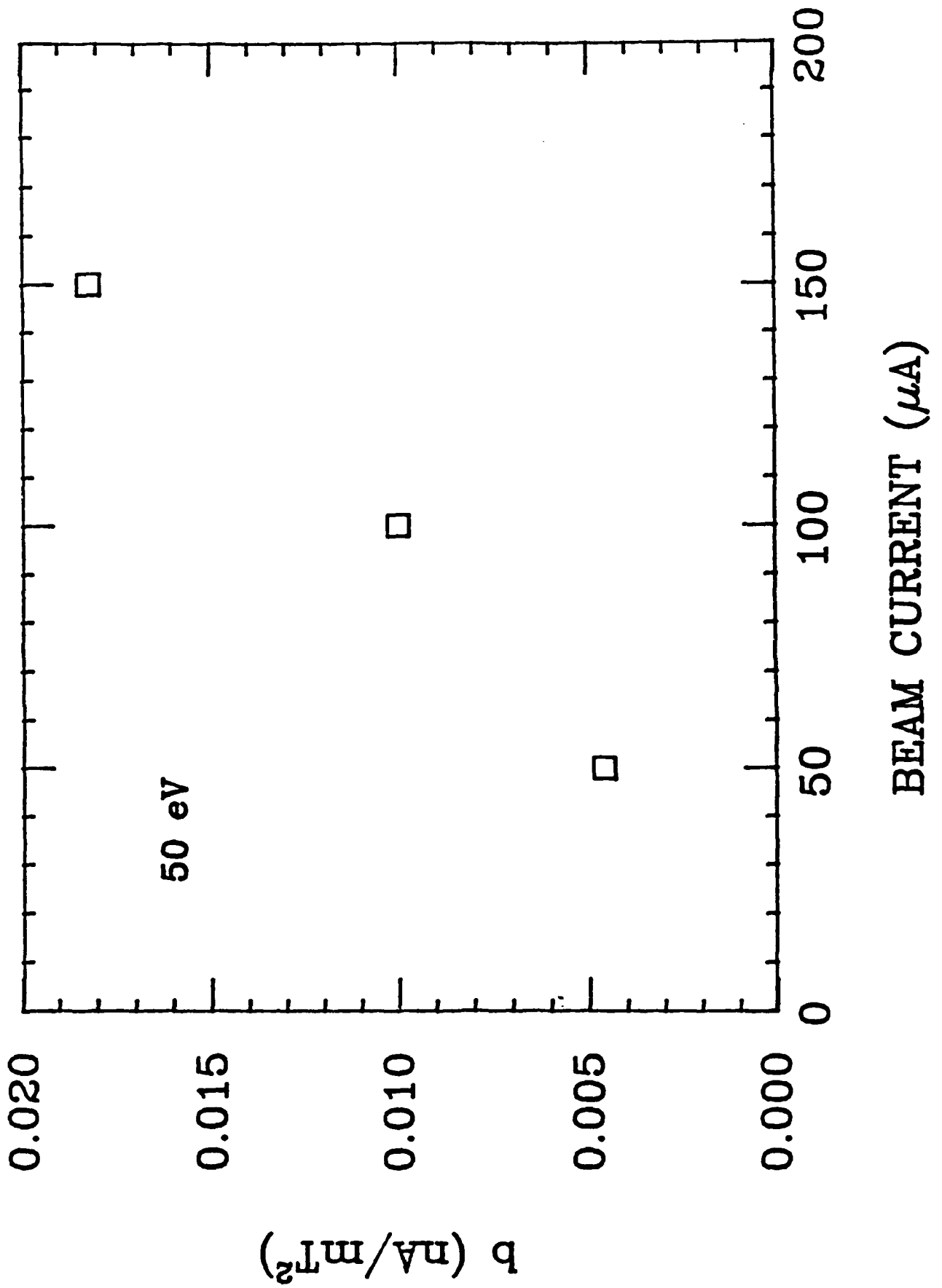


Figure 9. Plot of coefficient  $b$  versus beam current at 50 eV.

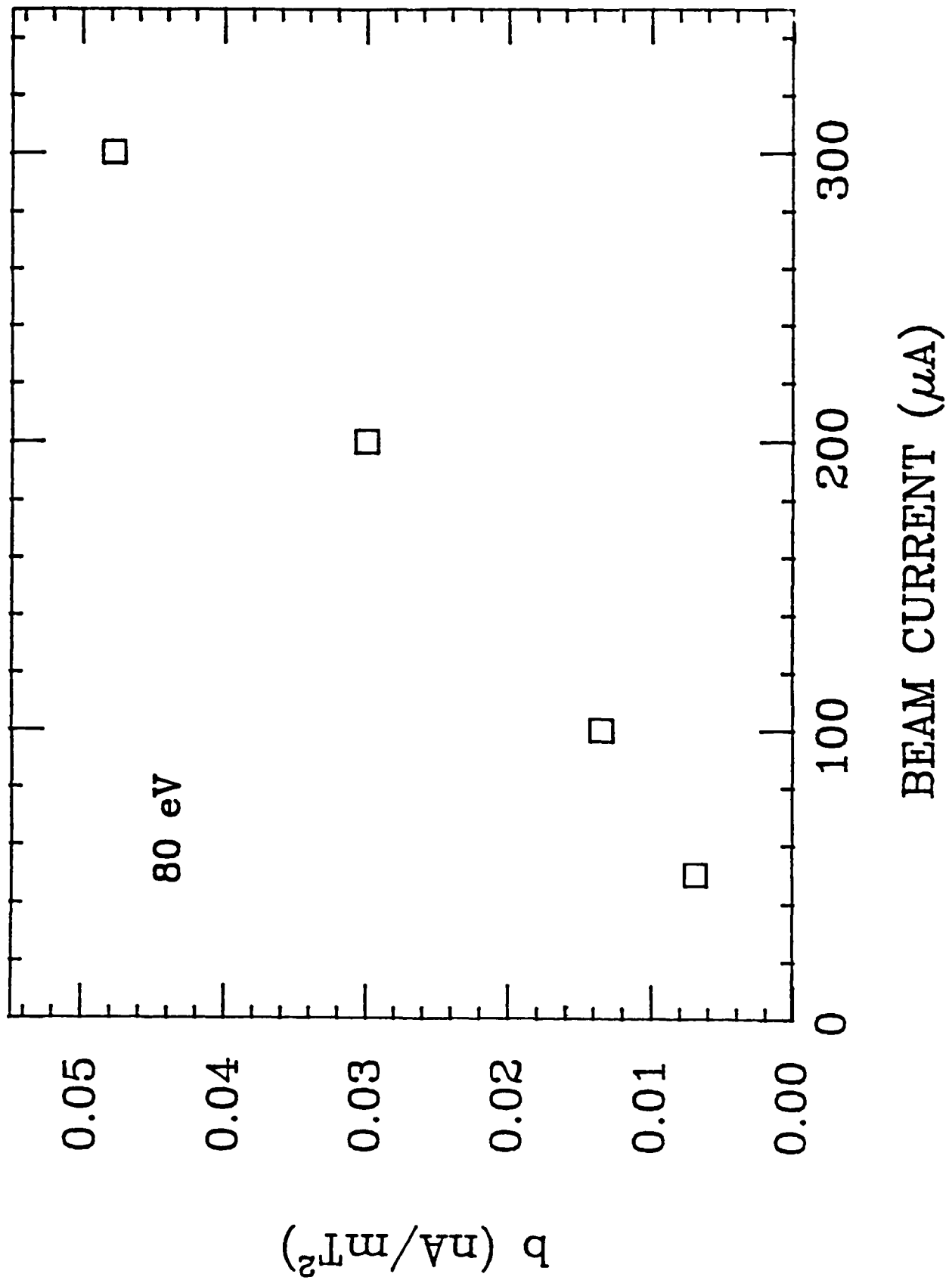


Figure 10. Plot of coefficient  $b$  versus beam current at 80 eV.

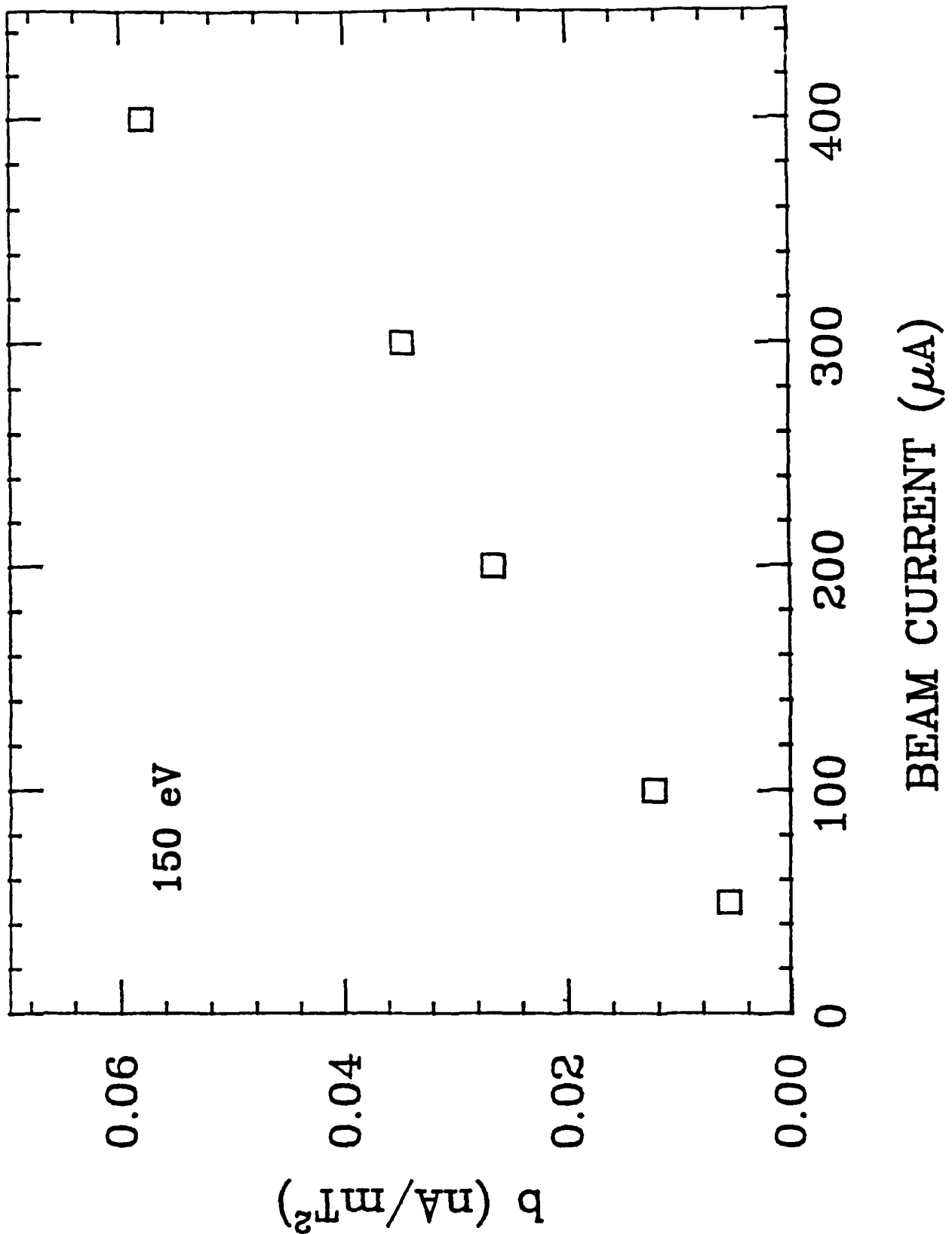


Figure 11. Plot of coefficient  $b$  versus beam current at 150 eV.

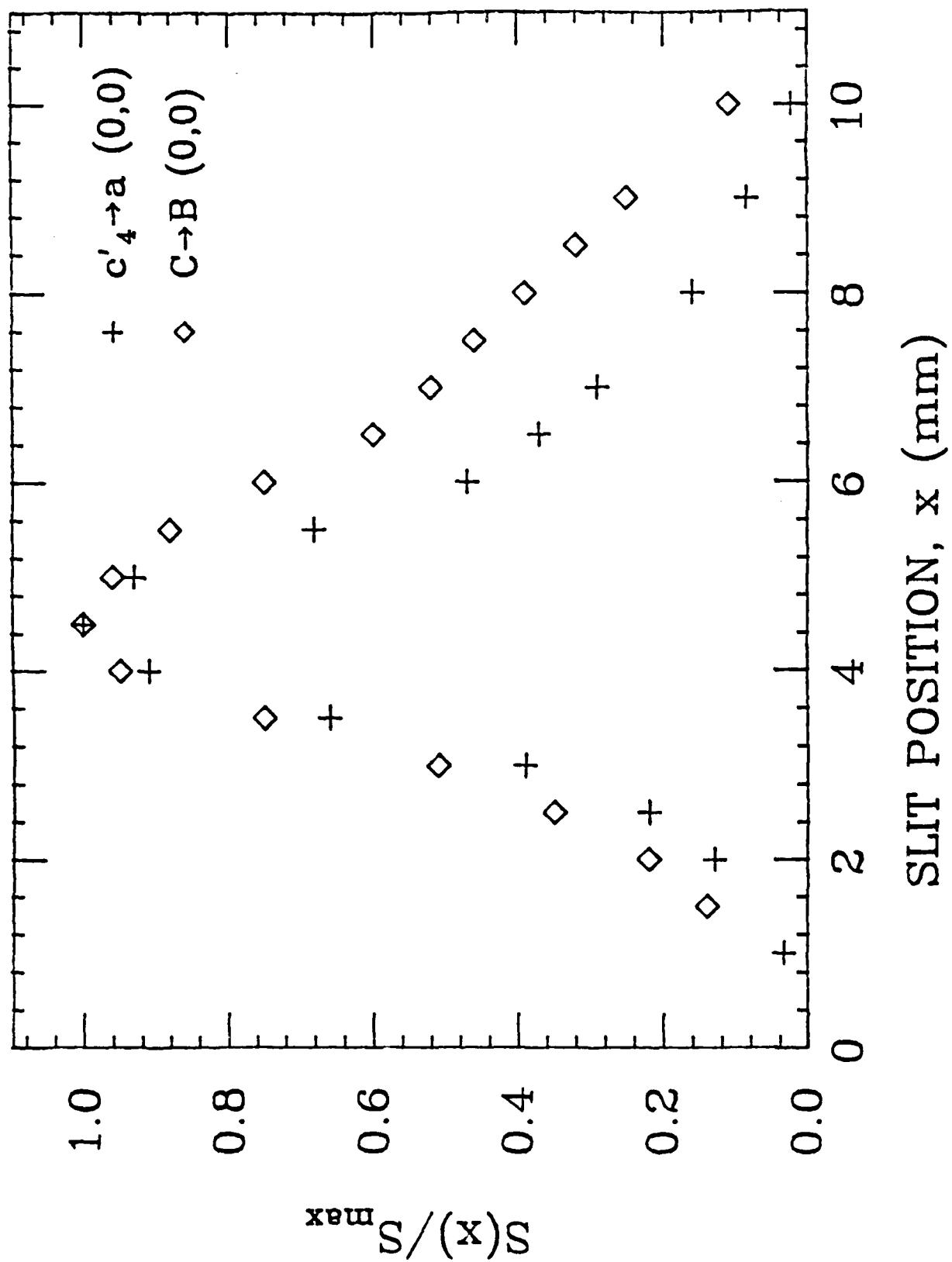


Figure 12. Intensity profile for the  $c'_4 \rightarrow a(0,0)$  and  $C \rightarrow B(0,0)$  bands.

energy of 100 eV with a monochromator bandpass of about 2.2 Å FWHM. For comparison we also measure the intensity profile for the C-B(0,0) band which is included in Fig. 11. We see that the  $c_4 \rightarrow a$  profile has a FWHM of 2.5 mm and lies well within the C-B profile of 4.2 mm FWHM. The  $C^3\Pi(v=0)$  state has a lifetime<sup>2</sup> of 37 nsec which is only somewhat longer than that of the  $c_4$  state. Therefore the intensity profile data do not show evidence of substantial cascade to the  $c_4$  state from long-lifetime states.

One reason for the strong interest in the  $c_4 \rightarrow a$  emission is that it is a source of population of the a-state which has a long radiative lifetime ( $10^{-4}$  sec). Long-living excited states play very prominent roles in energy transfer. Dynamical processes relevant to the population and depopulation of such excited states are of great importance. However, quantitative measurements are extremely difficult because of the low density of such excited species. Nevertheless in recent years significant progress has been made in experimental technique for studying long-living excited atoms in collision processes. For instance it is possible to measure number density of the neon atoms in the  $1s_5$  excited state generated by an electron beam through neon gas. In this kind of experiment it is convenient to work with a number density of  $1s_5$ -neon around  $10^9/\text{cm}^3$ . However, there are indications that such experiments can be run with a number density of the excited atoms as low as  $3 \times 10^6 \text{ cm}^{-3}$ . Furthermore extension of this technique allows one to measure the temporal growth and decay curve of the  $1s_5$ -neon atoms due to electron-beam excitation. It is also possible to use this technique to measure spatial variations of the density of the excited states. From these transient-type data, a decay time constant of 20  $\mu\text{sec}$  has been found. Another area of great importance is electron-impact excitation from a

long-living excited level (such as a metastable level) to a higher level. Very recently successful attempts have been made of experiments in which an electron beam is used to excite helium atoms in the  $2^3S$  level produced by a discharge (rather than by electron beam) to higher levels. Cross sections for electron-impact excitation of the  $2^3S$ -helium atoms to a number of higher states, including  $3^3S$ ,  $4^3S$ ,  $3^3P$ ,  $3^3D$ ,  $4^3D$ ,  $5^3D$ ,  $6^3D$ , have been obtained. There are also indications of cross section data for excitation from  $2^1S$  to  $3^1D$ ,  $4^1D$ ,  $4^1P$ . The use of a discharge is believed to produce more  $2^3S$ -helium atoms than the use of electron-beam excitation. However, when a discharge is used, the excited helium atoms and the electron beam for exciting the  $2^3S$ -helium atoms are not as well characterized and it was necessary to perform auxiliary experiments. To conduct similar studies for molecules is more difficult but should be extremely valuable. However, such experiments for probing excited atoms show great promise for extension to molecules.

#### References

1. A. R. Filippelli, S. Chung, and C. C. Lin, *Phys. Rev. A* 29, 1709 (1984).
2. A. Lofthus and P. H. Krupenie, *J. Phys. Chem. Rev. Data* 6, 113 (1977).

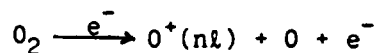
### Part III

#### EMISSION OF ATOMIC OXYGEN IONS RADIATION PRODUCED BY ELECTRON IMPACT ON OXYGEN MOLECULES

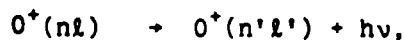
One of the most fundamental inelastic collision processes involving diatomic molecules is electron-impact dissociation. This occurs through excitation from the ground molecular electronic state to an unbound (repulsive) electronic state or the unbound portion of a partially bound state. Studies of this process allow us to probe into the collisional coupling of the various electronic states as well as the energy curves. Aside from the intrinsic interest, dissociative excitation is of great importance in many areas of applied physics and technology as it is a major mechanism for producing atoms from molecules. Specifically let us consider electrons colliding with oxygen molecules. Dissociative excitation of the molecules by electrons produces oxygen atoms and atomic oxygen ions in ground and excited states. Optical emission (or absorption) of these atoms and atomic ions provides us with a signature of these species. Measurements of the atomic emission lines may serve as a way to obtain information about the relevant processes. To use this technique effectively it is necessary to understand quantitatively how the excited atomic species are produced.

Studies of the emission lines of neutral oxygen atoms produced by electron-beam excitation of oxygen molecules have been reported in the literature, and measurements have been made for the optical emission cross sections of numerous neutral atomic-oxygen spectral lines.<sup>1</sup> Equally important is the formation of atomic ions by electron bombardment on  $O_2$  molecules, but very little is known about this dissociative ionization process especially when the  $O^+$  ions are produced in excited states. Let us denote an excited  $O^+$

ion in the  $1s^2 2s^2 2p^2 n\ell$  electron configuration by  $O^+(n\ell)$ . We focus our attention on the process,



(III-1)



and measured the optical emission cross sections for a series of  $O^+(n\ell \rightarrow n'\ell')$  transitions in the wavelength region of 2000-8000Å produced by electron impact on  $O_2$ . The experimental method is similar to that described in Part I of this report and has been described in the literature.<sup>1,2</sup> A beam of monoenergetic electrons is generated by an electron gun and passes through a collision chamber containing research grade oxygen gas at a pressure about a few mTorr. The  $O^+$  emission is viewed perpendicular to the electron beam, spectrally resolved by a monochromator, and converted to a proportional current by a photomultiplier. Absolute calibration of radiation intensity is made by means of standard lamps (tungsten lamp and/or deuterium lamp). The apparatus and experimental procedure have been fully described in the papers cited above and will not be repeated here. To facilitate spectral identification we have studied the  $O^+$  emission lines produced in a discharge. The discharge gives much more intense radiation than does the electron-beam collision chamber. We find the discharge spectrum to be a useful guide for studying  $O^+$  radiation emitted by electron-beam excitation.

The cross sections for the various  $O^+$  emission lines at an incident electron energy of 200 eV are listed in Table II. In Figure 13 is shown the

Table II. Electron-impact optical emission cross sections  $Q$  for  $0^+$  transitions of wavelength  $\lambda$  at 200 eV.

$n_2LS \rightarrow n_1l_1'l_1'S'$	$J \rightarrow J'$	$\lambda$ (in Å)	$Q$ (in $10^{-20} \text{cm}^2$ )
$3p^4S - 3s^4P$	$3/2 - 3/2$	3727	1.8
	$3/2 - 5/2$	3749	2.1
$3p^4P - 3s^4P$	$3/2 - 1/2$	4317	1.1
	$5/2 - 3/2$	4320	1.3
$3p^4D - 3s^4P$	$3/2 - 1/2$	4639	2.9
	$5/2 - 3/2$	4642	7.0
	$7/2 - 5/2, 1/2 - 1/2$	4649	17.0
	$3/2 - 3/2$	4661	3.2
	$5/2 - 5/2$	4676	2.2
$3d^4D - 3p^4D$	$7/2 - 7/2, 5/2 - 7/2$	3882	1.6
$3d^4D - 3p^4P$	$7/2 - 5/2, 5/2 - 5/2, 3/2 - 5/2$	4119	2.4
	$5/2 - 3/2, 3/2 - 3/2, 1/2 - 1/2$	4105	0.35
$3d^4F - 3p^4D$	$3/2 - 1/2, 5/2 - 3/2$	4070	4.7
	$7/2 - 5/2$	4072	5.1
	$9/2 - 7/2$	4076	5.2
$4p^4D - 3d^4F$	$7/2 - 9/2$	6895	1.6
$4f^4D - 3d^4P$	$7/2 - 5/2$	4304	1.1
	$5/2 - 3/2$	4294	0.64

$3p^2P - 3s^2P$	$3/2 - 3/2$	3973	3.3
	$1/2 - 3/2$	3983	0.76
$3p^2D - 3s^2P$	$5/2 - 3/2$	4415	6.7
	$3/2 - 1/2$	4417	4.7
$4f^2F - 3d^2D$	$5/2 - 3/2$	4602	0.4
$3p^12F - 3s^12D$	$7/2 - 5/2$	4591	3.8
	$5/2 - 3/2$	4596	2.4
$3d^12G - 3p^12F$	$9/2 - 7/2$	4190	3.4
	$7/2 - 5/2$	4185	3.6

---

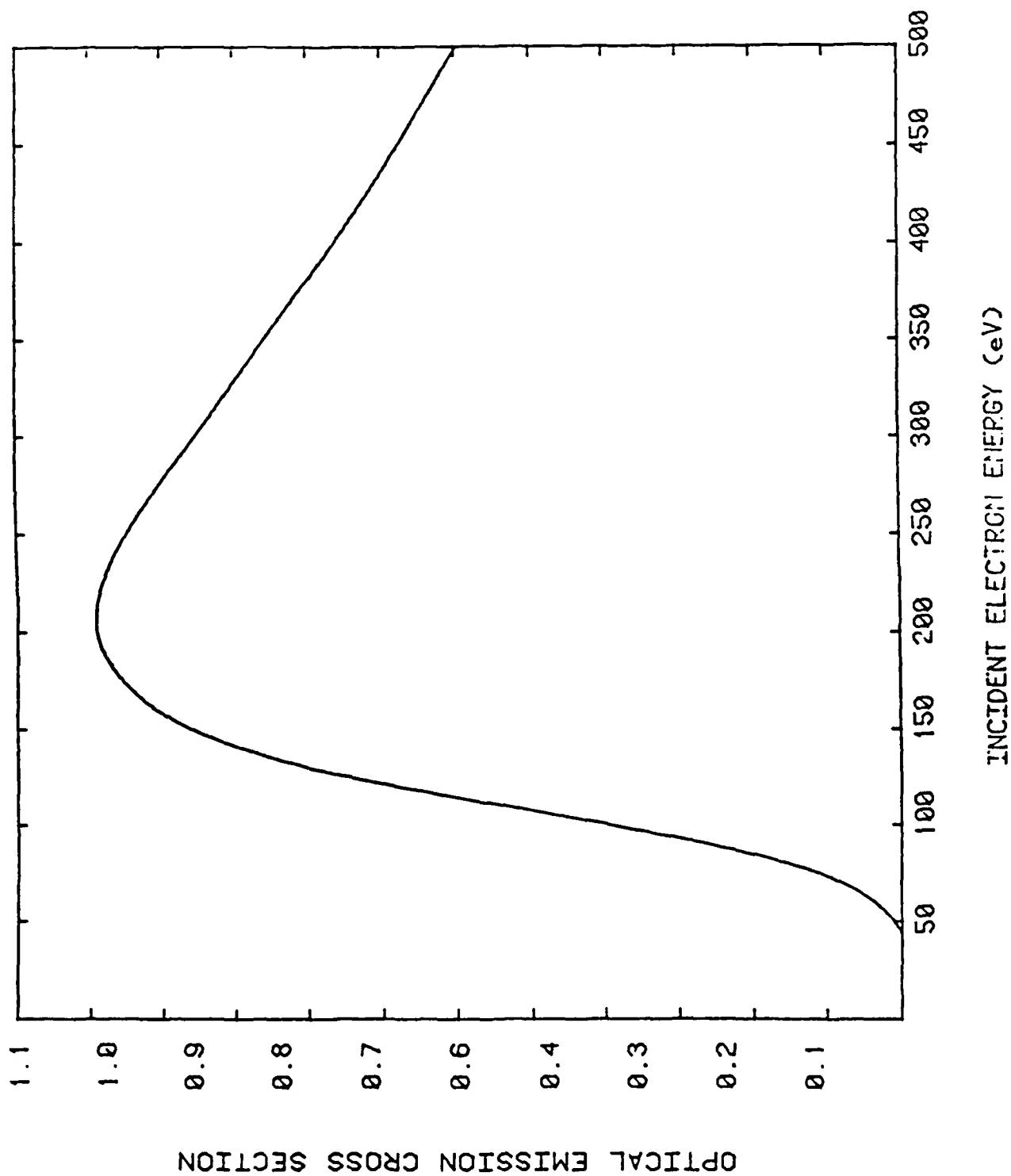


Figure 13. Electron-impact excitation function for the emission of the 4650 Å line of  $O^+$ .

excitation function (cross section as a function of the incident electron energy) for a typical  $O^+$  emission line.

Consider two emission transmissions,  $i \rightarrow j$  and  $i \rightarrow k$ , that originate from the same upper level  $i$ . The photon emission intensity ( $I$ ) is equal to the number density of atoms in the  $i$ -th state ( $N_i$ ) times the appropriate transition probability ( $A$ ), i.e.,

$$I(i \rightarrow j) = N_i A(i \rightarrow j), \quad (\text{III-2})$$

$$I(i \rightarrow k) = N_i A(i \rightarrow k). \quad (\text{III-3})$$

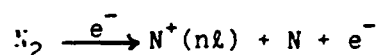
Since the optical emission cross section ( $Q$ ) is directly proportional to the photon emission intensity, we have

$$\frac{Q(i \rightarrow j)}{Q(i \rightarrow k)} = \frac{A(i \rightarrow j)}{A(i \rightarrow k)}. \quad (\text{III-4})$$

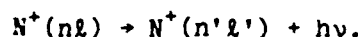
Suppose that  $i \rightarrow j$  is a transition of wavelength 2000-8000Å for which the emission cross section has been measured and that  $i \rightarrow k$  is a transition in the far infrared for which direct measurement of  $Q(i \rightarrow k)$  is not possible because of the very low sensitivity of the infrared detectors (as compared to photomultipliers). From the preceding equation we can obtain  $Q(i \rightarrow k)$  from the measured  $Q(i \rightarrow j)$  and the two transition probabilities involved. We have developed schemes for calculating atomic transition probabilities involving high excited states using an approximate treatment for exchange and using a Hartree-Fock method with configuration interaction. In particular, we have calculated transition probabilities for a large number of  $O^+$  lines using a Hartree-Fock method with configuration interaction. Using these transition

probabilities we obtain the emission cross section for the infrared transition  $4f^2D \rightarrow 4d^4P$  ( $\lambda=15$  microns) as  $2.1 \times 10^{-24}$  cm<sup>2</sup> at 200 eV, and the cross section for the infrared transition  $4f^2F \rightarrow 4d^2D$  ( $\lambda=38$  microns) as  $3.1 \times 10^{-26}$  cm<sup>2</sup>.

To gain a more complete picture of the production of  $O^+$  emission by electron impact on oxygen molecules, we compare it with the corresponding process for nitrogen,



(III-5)



We have analyzed the measured cross sections for emission lines of  $N^+$  ions produced by electron impact on  $N_2$ . The excitation functions for all the emission lines show a broad peak at 190 eV. Near the threshold energy the excitation function increases gently with an initial slope of nearly zero. Within a multiplet ( $n\ell LS \rightarrow n'\ell' L'S'$ ), the relative intensity of the various  $J \rightarrow J'$  transitions is consistent with a simple theoretical model in which the population of a  $J$ -level within an  $n\ell LS$ -manifold is proportional to the statistical weight  $2J+1$ . The peak cross section for the more intense multiplets of  $N^+$  is as large as  $16 \times 10^{-20}$  cm<sup>2</sup>. In addition to transitions of the type  $(2s^2 2p)n\ell \rightarrow (2s^2 2p)n'\ell'$ , we have also observed transitions in which the active electron ( $n\ell$ ) is associated with a core in the excited state. All these observations are in accordance with the features exhibited in our  $O^+$  emission cross section data. For the case of  $N^+$  emission data, the excitation functions of some of the emission lines exhibit a discontinuity in slope at energy around 85 eV which is suggestive of addition of new channels for

producing  $N^+(nl)$ . Such a discontinuity in slope has not been found in our  $O^+$  data.

Of all the  $N^+$  emission transitions that we have studied, the  $3p^3D + 3s^3P$  multiplet has the largest cross section ( $16 \times 10^{-20} \text{ cm}^2$  at 200 eV). The  $3d^3F + 3p^3D$  multiplet also has a large cross section,  $14 \times 10^{-20} \text{ cm}^2$ . The cross sections in the singlet family are smaller, i.e.,  $5.2 \times 10^{-20} \text{ cm}^2$  for  $3p^1P + 3s^1P$  and  $0.22 \times 10^{-20} \text{ cm}^2$  for  $3d^1D + 3p^1P$ . The majority of the  $N^+$  multiplet cross sections are below  $10^{-20} \text{ cm}^2$ . For example  $4p^1S + 3d^1P$ ,  $4p^1P + 3d^1D$ ,  $4p^1D + 3d^1F$ ,  $3d^3D + 3p^3P$ ,  $4p^3P + 3d^3D$  all have cross sections no larger than  $0.5 \times 10^{-20} \text{ cm}^2$ . We have observed four multiplets involving the  $3s'$ ,  $3p'$ ,  $3d'$  states ( $3p'^3P + 3s'^3P$ ,  $3p'^5S + 3s'^5P$ ,  $3d'^5P + 3p'^5P$ ,  $3d'^5D + 3p'^5P$ ). Their cross sections are below  $0.4 \times 10^{-20} \text{ cm}^2$ . The  $N^+$  cross sections cited above are all at 200 eV. In contrast we see that all the  $O^+$  cross sections given in Table II, with four exceptions, are all larger than  $10^{-20} \text{ cm}^2$ . Moreover, the cross sections in Table II refer to individual J-components. The cross sections would be even larger if they were expressed as multiplet cross sections.

It was pointed out in Refs. 1, 3, 4 that for production of neutral atomic O (or N) emission by electron impact on  $O_2$  (or  $N_2$ ), the observed threshold energy is nearly equal to the energy defect (within experimental uncertainty). On the other hand, our measurements for both  $O^+$  and  $N^+$  emission show a threshold energy several eV higher than the energy defect. This signifies a fundamental difference in the production mechanism between  $O^+$  (or  $N^+$ ) emission and O (or N) emission. For illustration let us consider the formation of an excited N atom ( $N^*$ ) by electron impact on  $N_2$ . This proceeds through the intermediary of an excited  $N_2$  molecule ( $N_2^*$ ) followed by dissociation, i.e.,



In Fig. 14 we show schematically the energy curves (electronic energy versus internuclear distance) of  $N_2$  and  $N_2^*$ . According to the Franck-Condon principle, process (III-6) from the lowest vibrational level of the  $N_2(X^1\Sigma_g^+)$  electronic state proceeds "vertically" within the Franck-Condon region which is represented by the shaded area in Fig. 14. Let us first assume that the  $N_2^*$  state is of  $\alpha$ -type which is defined as either a purely repulsive electronic state (shown in Fig. 13) or a bound electronic state for which the left-hand classical turning point of the highest bound vibrational level is outside (to the right of) the shaded area (not shown in Fig. 14). A vertical excitation from  $N_2(X^1\Sigma_g^+)$  to an  $\alpha$ -type  $N_2^*$  state is illustrated by path (a) in Fig. 14. The threshold energy corresponds to excitation along the right-hand edge of the Franck-Condon region and is shown in Fig. 14 as  $(E_{th}^*)_{\alpha}$  which is obviously larger than the energy defect,  $\Delta E$ , shown in the same graph. Next we assume that  $N_2^*$  is of  $\beta$ -type which is defined as a bound state for which the left-hand classical turning point of the highest bound vibrational level is inside the shaded area as shown in Fig. 14. Here excitation from  $N_2(X^1\Sigma_g^+)$  to the  $\beta$ -type  $N_2^*$  through the vertical path (b) as shown in Fig. 14 corresponds to threshold excitation, and it is clear that in this case the threshold energy is equal to the energy defect,  $\Delta E$ . Thus comparing the observed threshold energy with the energy defect, we see that for production of neutral N emission, the excitation process (III-6) proceeds through a  $\beta$ -type intermediate state  $N_2^*$ . Likewise for production of neutral O emission, the electro-impact process

ELECTRONIC ENERGY

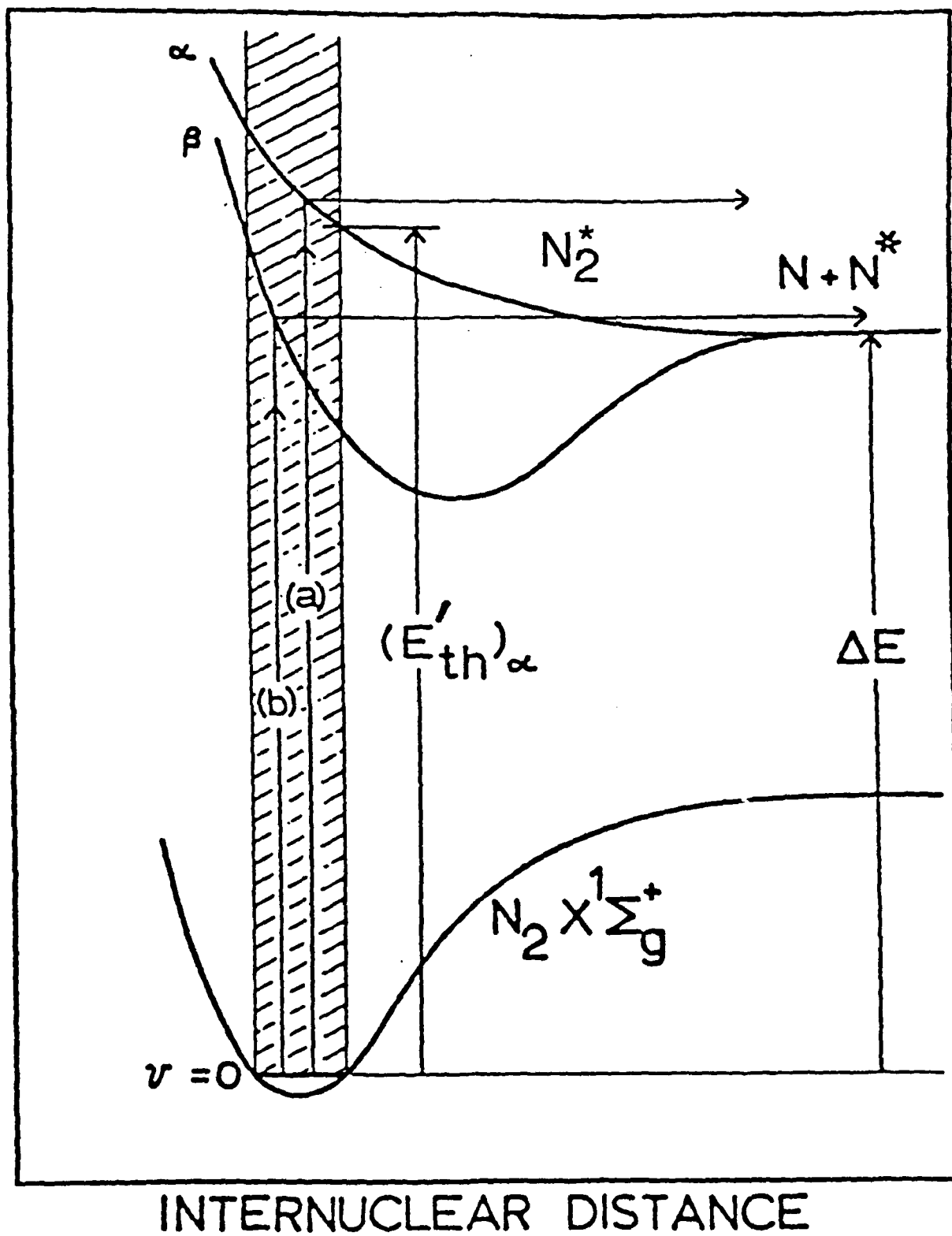


Figure 14. Schematic diagram of energy curves relevant to electron-impact dissociation.

proceeds through a  $\beta$ -type intermediate  $O_2^*$  state. On the other hand for production of  $N^+$  (or  $O^+$ ) emission, because the threshold energy is several eV larger than the energy effect, we conclude that key electron impact process is



where  $N_2^{+*}$  (or  $O_2^{+*}$ ) is an  $\alpha$ -type state. This is illustrated in Fig. 15 by path (a).

ELECTRONIC ENERGY

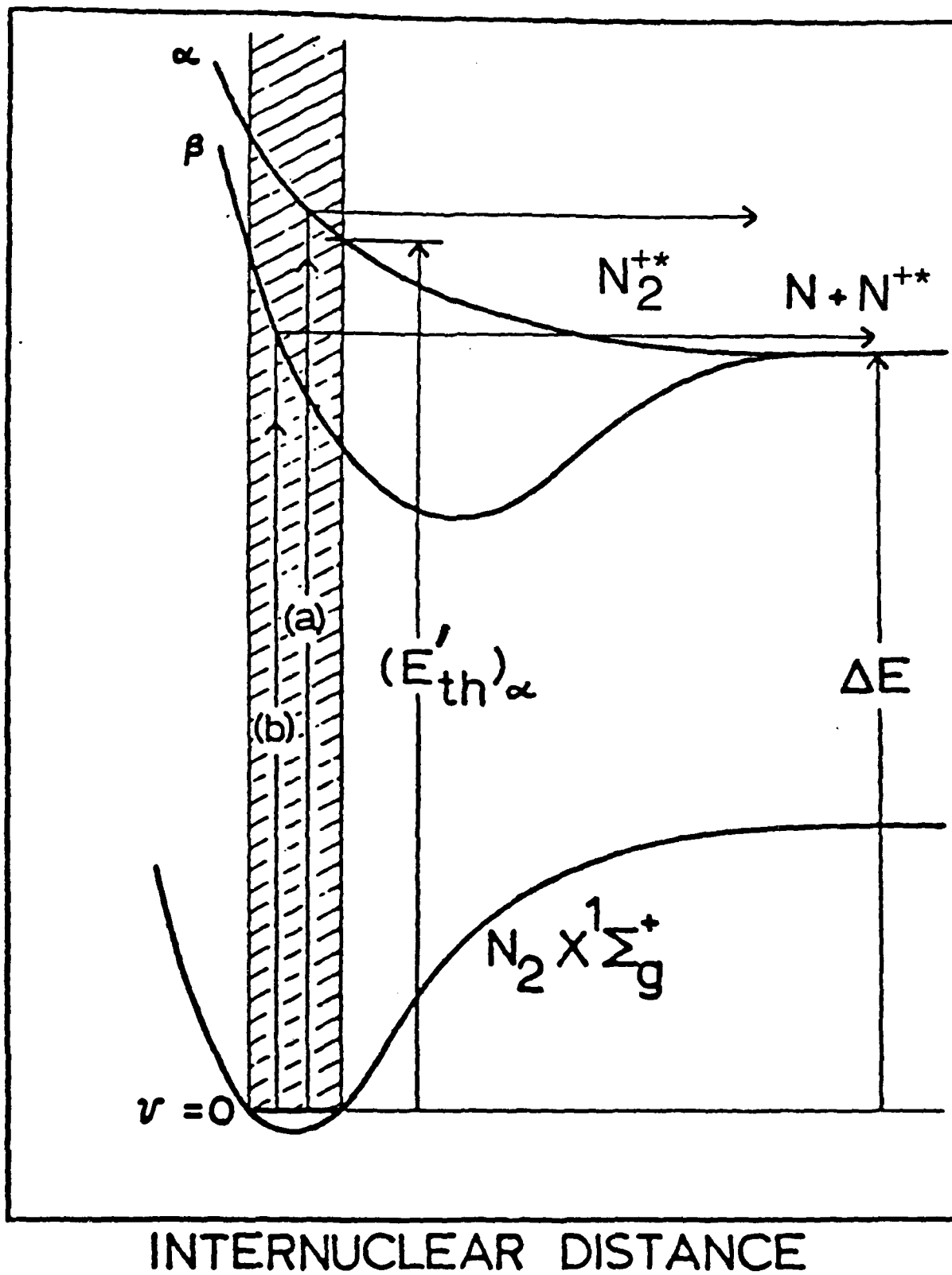


Figure 15. Schematic diagram of energy curves relevant to electron-impact dissociative ionization.

#### REFERENCES

1. M. B. Schulman, F. A. Sharpton, S. Chung, C. C. Lin, and L. W. Anderson, Phys. Rev. A 32, 2100 (1985).
2. A. R. Filippelli, S. Chung, and C. C. Lin, Phys. Rev. A 29, 1709 (1984).
3. D. L. A. Rall, A. R. Filippelli, F. A. Sharpton, S. Chung, C. C. Lin, R. E. Murphy, J. Chem. Phys. 87, 2466 (1987).
4. A. R. Filippelli, F. A. Sharpton, C. C. Lin, R. E. Murphy, J. Chem. Phys. 76, 3597 (1982).

PUBLICATIONS

S. Chung, C. C. Lin, and E. Lee, "Transition Probabilities of Spectral Lines of Singly Ionized Atomic Oxygen (OII)", J. Quant. Spectrosc. Radiat. Transfer, to be published.

D. L. A. Rall, F. A. Sharpton, and C. C. Lin, "Excitation of Emission Lines of Atomic Nitrogen Ions by Electron-Impact Dissociative Ionization of Nitrogen Molecules", submitted to the Journal of Chemical Physics.

J. S. Allen and C. C. Lin, "Electron-Impact Excitation of the Vibrational Levels of the  $c_4^1\Sigma_u^+$  State of the Nitrogen Molecule", submitted to the Physical Review.

K. A. Jackson and C. C. Lin, "Multiplet-Dependent Wave Functions from the Local Spin Density Approximation with Self-Interaction Correction", submitted to the Physical Review.